Oxidation of CO, ethanol and toluene over TiO_2 supported noble metal catalysts

Vera P. Santos [a], Sónia A.C. Carabineiro [a], Pedro B. Tavares [b], Manuel F.R. Pereira [a], José J.M. Órfão [a], José L. Figueiredo [a,*]

[a] *Laboratório de Catálise e Materiais (LCM), Laboratório Associado LSRE/LCM, Faculdade de Engenharia, Universidade do Porto, Rua Dr. Roberto Frias, s/n, 4200-465 Porto, Portugal*
[b] *Centro de Química de Vila Real (CQVR), Universidade de Trás-os-Montes e Alto Douro, Departamento de Química, 5001-911 Vila Real, Portugal*

ARTICLE INFO

ABSTRACT

The oxidation of CO, ethanol and toluene was investigated on noble metal catalysts (Pt, Pd, Ir, Rh and Au) supported on TiO_2. The catalysts were prepared by liquid phase reduction deposition (LPRD) and by incipient wetness impregnation (IMP). It was observed that the preparation method can have a significant effect on the dispersion of the metallic phase, and subsequently on the performance of the catalysts towards total oxidation of CO or VOC.

For CO oxidation, Au IMP was the worst catalyst, while Au LPRD was the most active. This can be explained in terms of different Au particle sizes, well known to be related with catalytic activity. For all the other metals, LPRD also produces better results, although the differences are not so marked as with gold. Iridium seems to be the only exception since results were very similar.

In VOC oxidation, the following performance trend was observed: $Pt/TiO_2 > Pd/TiO_2 \gg Rh/TiO_2 \approx Ir/TiO_2 \gg Au/TiO_2$, for both preparation methods. Ethanol and toluene oxidation over Pt and Pd catalysts were found to be structure sensitive reactions.

Some experiments with ethanol/toluene mixtures were performed using the best catalyst (Pt/TiO_2). It was observed that toluene inhibits the combustion of ethanol, namely by slowing down the partial oxidation of ethanol towards acetaldehyde. Ethanol also has a slight inhibition effect on the total oxidation of toluene.

1. Introduction

The design of catalytic systems for the reduction of polluting emissions is an important tool for environmental protection. Supported noble metal catalysts are well known for their high activity in oxidation reactions [1–13]. It has been established for a long time that the catalytic activity and/or the selectivity of noble metals (especially gold) strongly depends on the particle size and this parameter is a function of several factors, including the preparation method. For example, gold is only active when it is deposited as ultrafine particles with high dispersion on metal oxide supports, which is not accomplished by the conventional preparation methods, such as traditional impregnation [9,12,13]. The problem of these methods is that they generally lead to poorly active systems due to the presence of chloride, which is well known to

cause sinterization of gold particles, thus turning them inactive [9,12–14].

There is an extensive work concerning the oxidation of VOC and CO over supported noble metal catalysts [1,3,7,9,12,13,15]. Most of these studies involve supported Pt, Pd or Au [9,12,13,15–19], titania being one of the most widely used carriers.

As CO is a possible by-product in VOC oxidation (as not always complete oxidation of the pollutant to CO_2 takes place), the study of CO oxidation is also important in this context. As documented in the literature, this reaction follows a Langmuir–Hinshelwood mechanism, over noble metal catalysts (Pt, Pd), and the surface reaction occurs between adsorbed CO and dissociatively adsorbed oxygen. On supported Au catalysts the reaction mechanism is more complex, and it is widely accepted that a CO molecule is chemisorbed on a gold atom, while an hydroxyl ion moves from the support to an Au(III) ion, creating an anion vacancy. They react to form a carboxylate group, and an oxygen molecule occupies the anion vacancy as O_2^-. This oxidizes the carboxylate group by extracting a hydrogen atom, forming carbon dioxide, and the resulting hydroperoxide ion HO_2^- then oxidizes a further carboxylate species forming another carbon dioxide and restoring

* Corresponding author. Tel.: +351 22 5081 663; fax: +351 22 5081 449.
E-mail addresses: santos.vera@fe.up.pt (V.P. Santos), sonia.carabineiro@fe.up.pt (S.A.C. Carabineiro), ptavares@utad.pt (P.B. Tavares), fpereira@fe.up.pt (M.F.R. Pereira), jjmo@fe.up.pt (J.J.M. Órfão), jlfig@fe.up.pt (J.L. Figueiredo).

two hydroxide ions on the support surface, completing the catalytic cycle. This mechanism was proposed in 2000 by Bond and Thompson [9], and has been substantiated by subsequent results [20].

On the other hand, it is generally accepted that the oxidation of VOC over noble metals involves the dissociative adsorption of oxygen, followed by a Langmuir–Hinshelwood mechanism (reaction with chemisorbed reactant) or a Rideal–Eley mechanism (reaction with gaseous reactant), depending on the nucleophilic character of the particular organic reactant [1]. In some metals, such as Ag, oxygen chemisorption is too strong, which implies a Mars–van Krevelen mechanism similar to metal oxides (with formation of surface oxygen vacancies as the key step and their successive replenishment by gas-phase oxygen) [1].

Another important aspect concerning the oxidation of VOC over noble metal catalysts is that the reaction is generally recognized to be structure sensitive. The effect of the Pt particle size on the catalytic combustion of different hydrocarbons has been extensively studied [21–23]. Nevertheless, the results obtained are conflicting, probably due to the fact that the correlation between catalytic activity and metal dispersion depends on the type of VOC. Very few papers deal with the structure sensitivity of aromatic hydrocarbons combustion on Pt-based catalysts. Papaefthimiou et al. [3] studied the oxidation of benzene over Pt-based catalysts. They found that, in the presence of Pt-Al$_2$O$_3$, turnover rates strongly increase with increasing Pt particle size.

It is well known that the preparation method is crucial to obtain catalysts with small particle sizes, especially for gold supported catalysts [9,12,13]. The liquid phase reduction deposition (LPRD) method was used by Sunagawa et al. [24] to prepare Pt and Au catalysts supported on Fe$_2$O$_3$, FeOOH, ZrO$_2$ and TiO$_2$, and by our group for the preparation of Au/ceria catalysts for CO oxidation [14]. This technique is based on the adsorption of metal ions or complexes on the surface followed by reduction. The initial adsorption of metal or complexes is thus the key point of this method. Highly dispersed particles on the support can be produced, overcoming the limitations of the conventional methods (incipient wetness impregnation and ion exchange) [24].

In the present work, several noble metals (Pt, Pd, Rh, Ir and Au) were supported on commercial titania by LPRD and by traditional incipient wetness impregnation (IMP). The materials were characterized by transmission electron microscopy (TEM) and pulse chemisorption of hydrogen, and used as catalysts for the oxidation of CO, ethanol, toluene and mixtures of these two VOC. The influence of the preparation method and the type of metal on the catalytic activity was assessed.

To the best of our knowledge, there are no reports in the literature dealing with catalytic oxidation of toluene and ethanol, where a comparison of several noble metals supported on titania prepared by the two different methods mentioned above is made. Particularly, we found no reference to studies concerning titania supported Ir or Rh catalysts for VOC oxidation.

2. Experimental

2.1. Catalysts preparation and characterization

Commercial TiO$_2$ (Degussa P 25) was used as support. Supported noble metal (Pt, Pd, Ir, Rh and Au) catalysts were prepared by incipient wetness impregnation (IMP) and liquid phase reduction deposition (LPRD) with 1% metal load (nominal). These catalysts are referred to in subsequent text as M IMP and M LPRD, where M defines the noble metal.

In the first method, an appropriate volume of the corresponding precursor (see Table 1) was added to the support. The resultant materials were dried at 110 °C overnight and calcined at 500 °C for 2 h.

The second method (LPRD) consists of mixing a solution of the precursor with a solution of NaOH with stirring at room temperature. The resulting solution is aged for 24 h, in the dark, at room temperature to complete the hydroxylation. Then the appropriate amount of support is added to the solution and, after ultrasonic dispersion for 30 min, the suspension is aged in the oven at 100 °C overnight. The resulting solid is washed repeatedly with distilled water for chloride removal, and dried in the oven at 100 °C overnight.

The metal dispersion was determined by hydrogen chemisorption with an Altamira instrument (AMI 200). The samples were pre-reduced at 400 °C in a stream of hydrogen and then cooled to room temperature, in order to proceed with the pulse chemisorption of hydrogen. For palladium catalysts, metal dispersions were obtained by chemisorption at 70 °C, in order to avoid the formation of β-Pd hydride phase by diffusion of hydrogen into the palladium [25]. In fact, measurements carried out with Pd samples at room temperature gave lower dispersions, as will be discussed ahead.

The average metal particle sizes were determined also by transmission electron microscopy (TEM) using a Leo 906 E apparatus, at 100 kV. Samples were prepared by ultrasonic dispersion in ethanol and placed on a copper grid for TEM analysis.

The noble metal loading of the samples was determined by inductively coupled plasma–optical emission spectroscopy (ICP/OES) in an external laboratory.

2.2. Catalytic experiments

2.2.1. CO oxidation

CO oxidation experiments were performed using a continuous flow reactor. The catalyst sample weight was 200 mg and the feed gas (5% CO, 10% O$_2$ in He) was passed through the catalytic bed at

Table 1
Properties of TiO$_2$ supported catalysts (D_M – metal dispersion, d_M – average diameter of the metal particles).

Catalyst	Precursor	Metal loading (%)	D_M (%)[a]	d_M (nm)[a]	D_M (%)[b]	d_M (nm)[b]
Pt IMP	H$_2$PtCl$_6$·6H$_2$O	0.8	19	5.4	16	6.3
Pd IMP	PdCl$_2$	0.9	16[c]	7.2[c]	14	8.0
Ir IMP	H$_2$IrCl$_6$·H$_2$O	0.3	60	1.9	–	–
Rh IMP	RhCl$_3$·3H$_2$O	0.8	21	5.2	14	7.9
Au IMP	HAuCl$_4$·3H$_2$O	0.9	–	–	13	9.1
Pt LPRD	H$_2$PtCl$_6$·6H$_2$O	1.1	28	3.6	–	–
Pd LPRD	PdCl$_2$	1.1	28[c]	4.0[c]	38	3.0
Ir LPRD	H$_2$IrCl$_6$·H$_2$O	0.9	64	1.7	–	–
Rh LPRD	RhCl$_3$·3H$_2$O	1.1	29	3.8	–	–
Au LPRD	HAuCl$_4$·3H$_2$O	0.5	–	–	29	4.0

[a] Obtained by hydrogen chemisorption at room temperature.
[b] Obtained by TEM.
[c] Obtained by hydrogen chemisorption at 70 °C (see text for details).

a total flow rate of 50 N cm^3 min^{-1}. The reaction temperature was raised from room temperature until full conversion was obtained, by steps of 25 °C. The reactor was maintained at each temperature for 20 min in order to obtain experimental values at steady state. The composition of the outgoing gas stream was determined by gas chromatography. Further details can be found elsewhere [14].

2.2.2. VOC oxidation

A different catalytic reactor was used for VOC oxidation. The catalytic oxidation of ethanol and toluene was carried under atmospheric pressure in a 6 mm stainless steel reactor (BTRS Jr Autoclave Engineers). A feed gas with a VOC concentration of 4000 mg C/m^3 and a space velocity of 16,000 h^{-1} was used in standard tests. The catalyst sample (0.05 g) was diluted with glass spheres of the same size as the catalyst particles ($0.2 < \phi < 0.5$ mm) (the total catalyst bed length was about 2 cm).

Conversions were measured over the range 100–300 °C in incremental steps (10–20 °C) and temperatures were measured by a thermocouple placed in the middle of the catalysts bed. To ensure the measurement of steady state data, the reactor was maintained at each temperature for 30 min. The conversion of VOC (X) and the conversion into CO_2 (X_{CO_2}) were respectively calculated as

$$X = 1 - \frac{F_{VOC}}{F_{VOC,in}} \quad \text{and} \quad X_{CO_2} = \frac{F_{CO_2}}{\nu F_{VOC,in}}$$

where F_{VOC} is the outlet molar flow rate of VOC at steady state, $F_{VOC,in}$ is the inlet molar flow rate of VOC, F_{CO_2} is the outlet molar flow rate of CO_2 at steady state and ν is the number of carbon atoms in the VOC molecule ($\nu = 2$ or 7, for ethanol or toluene, respectively). Further details can be found elsewhere [26].

The intrinsic activity (γ) was used in this work in order to compare the activity of the catalysts with different metal dispersions. γ was calculated as:

$$\gamma = \frac{F_{CO_2}}{w D_M / M}$$

where w is the metal weight, D_M is the metal dispersion and M is the molar mass of the noble metal.

3. Results and discussion

3.1. Catalyst characterization

The characteristics of the different catalysts are summarized in Table 1. As can be seen, the catalysts obtained by the two methods described above display very different metal particle sizes. When the metal is introduced by IMP, the average metal particle size ranges from 5 to 9 nm in all samples prepared, except for Ir (1.9 nm). The size is reduced to 2–4 nm when the metal is deposited by LPRD. As expected, highly dispersed noble metal catalysts were produced by this method (see Table 1), with values ranging from about 30% (for Pt, Pd, Rh and Au) to 64% (for Ir). IMP samples have lower dispersion, ranging from 13 to 21% for Pt, Pd, Rh and Au, and 60% for Ir. As mentioned in Section 2.1, the values for Pd dispersion were obtained by chemisorption at 70 °C, in order to avoid the formation of β-Pd hydrides. In fact, measurements carried out for the Pd LPRD sample at room temperature gave a lower dispersion (15%).

Fig. 1 shows selected TEM images of the titania supported catalysts prepared by both methods. It was not possible to obtain metal dispersions by TEM for Pt, Ir and Rh catalysts (prepared by LPRD) and Ir prepared by IMP, since no metal particles could be seen in the micrographs (not shown). This might be due to their very low sizes (most likely below detection limit of 2–3 nm). In fact, Table 1 shows that these catalysts present low average particle sizes
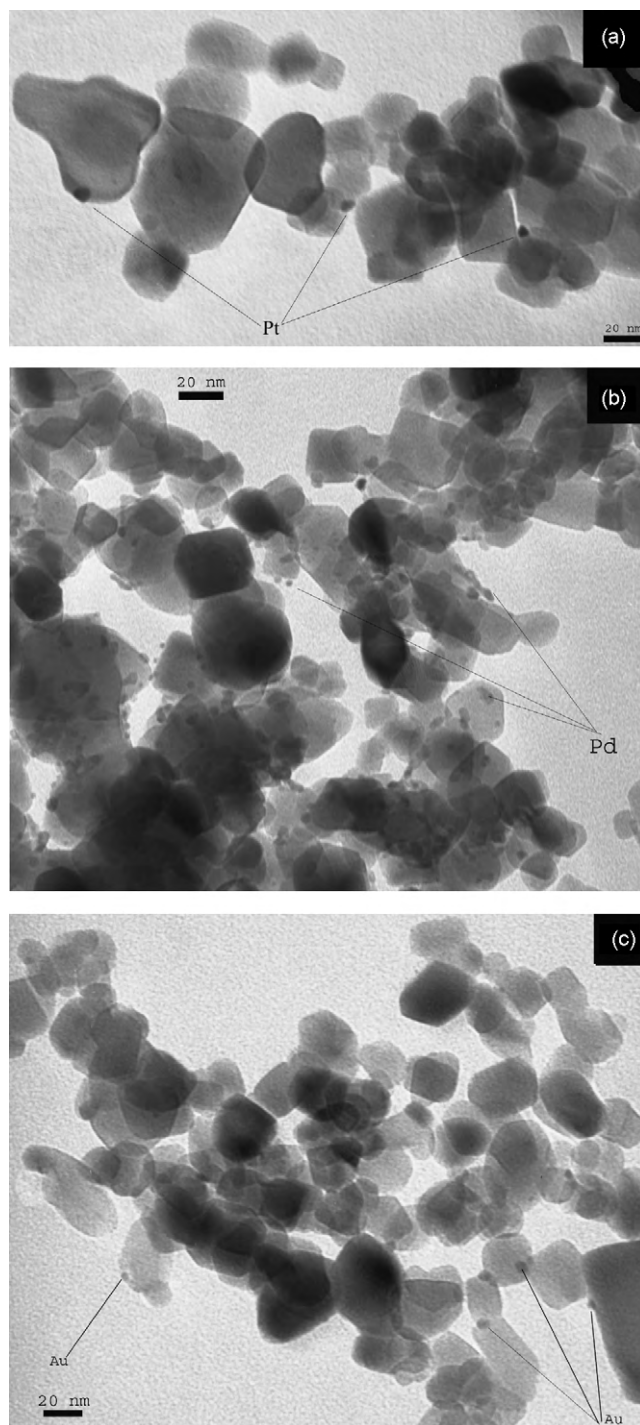

Fig. 1. TEM images of catalysts: (a) Pt IMP; (b) Pd LPRD; (c) Au LPRD.

($\sim$2–4 nm) determined by chemisorption (the experimental limitations imposed by the low metal loadings of about 1 wt% must be considered for this kind of technique). However, Pd particles can be seen very well (Fig. 1b). Catalysts prepared by IMP are also well visible (with the exception of Ir), since they show larger metal particle sizes (Fig. 1a is shown as an example). In general, there is a large difference between the particle sizes of catalysts prepared by IMP and LPRD methods, the latter producing much smaller particles (Fig. 1c, referring to Au LPRD catalyst, is shown as an example).

In the cases where comparison is possible, dispersions and particle sizes obtained by TEM and by hydrogen chemisorption are generally in agreement (although the latter method gives higher
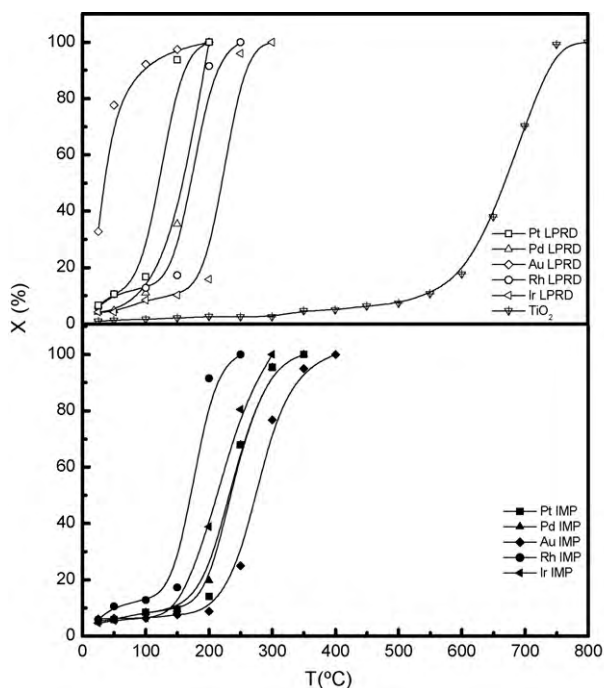
Fig. 2. Light-off curves for CO oxidation over supported noble metal catalysts.

Fig. 3. Volcano-type plot indicating the specific activity at 175 °C in CO oxidation for catalysts prepared by LPRD, as a function of oxygen dissociative chemisorption energies on metals.

values of dispersion), which implies that the majority of the metal particles are exposed on the titania surface.

The metal loading of the samples is also shown in Table 1. It can be observed that the Au contents resulting from the two preparation methods are quite different, ranging from 0.5% for LPRD to 0.9% for IMP. This result indicates that gold present in solution cannot be totally deposited on the support. It has been established that the preparation method has a strong influence on the metal loading. In fact, this is a common problem, as the gold loading depends on the way the metal is deposited on the surface, either in the form of a complex or in the reduced state [27–29].

3.2. Catalytic activities

All the catalysts studied in this work were tested in the oxidation of VOC (ethanol and toluene) and CO.

3.2.1. CO oxidation

Fig. 2 shows the light-off curves for CO oxidation with the titania supported catalysts, prepared by both methods, and with the support itself, for comparison. It can be observed that Au IMP is the worse catalyst of the group, while Au LPRD is by far the most active. This can be explained in terms of the particle sizes, well known to depend on the preparation method [9,12,13]. In fact, the IMP method, since it does not remove chloride, produces larger gold particles, which are much less active than the smaller produced by LPRD, as already shown with Au/ceria materials [14].

For all the remaining metals, LPRD still produces better results, although the difference is not so marked as with gold. Iridium seems to be the only exception, since both curves are very similar. The performance trend for LPRD samples is Au ≫ Pt > Pd > Rh > Ir, while for IMP samples the order Rh > Ir > Pd ≈ Pt > Au is observed. Particle sizes and metal dispersions alone are not enough to explain these differences; therefore they must be related with the metal itself. Thus, it should be interesting to plot the intrinsic activity of each noble metal at a selected temperature as a function of the dissociative chemisorption energies of oxygen [30], assuming
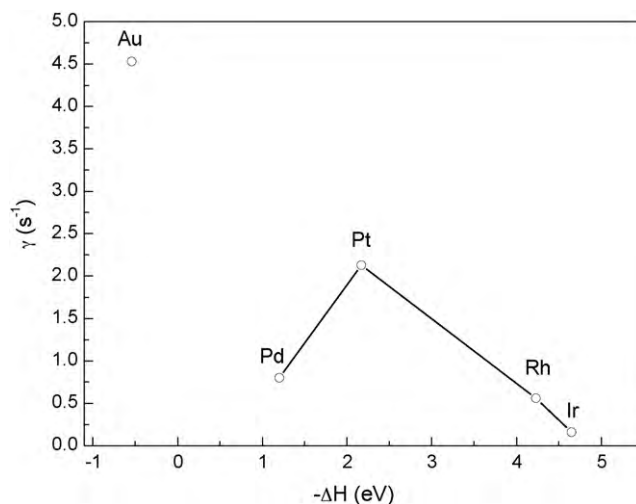
that dissociative adsorption of oxygen takes place. Fig. 3 shows the results obtained. If we disregard Au, since it presents a unique mechanism [9] (described in Section 1), a typical volcano plot occurs, explaining the catalytic trend observed.

3.2.2. VOC oxidation

Figs. 4 and 5 show the light-off curves for ethanol and toluene oxidation, respectively. For comparative purposes, the light-off curve of the support was also included. The temperatures corresponding to 50, 90 and 100% of conversion into CO_2 are summarized in Table 2. Accordingly, it can be observed that the temperature required for a certain level of conversion into CO_2 (higher than 50%), for both VOC studied, is always higher for the catalysts prepared by IMP, like the results obtained for CO oxidation. For example, with the Pt LPRD catalyst, ethanol and toluene are completely oxidized to CO_2 at 260 and 210 °C, respectively, which is ~20 °C less than with the Pt conventional catalyst (IMP). However, according to Table 1, the samples prepared by the two methods display very different metal dispersions, so their catalytic performance should be compared taking into account the particle size effect. The effect of the average metal particle size on the intrinsic activity (γ) of each catalyst is presented in Table 3. For each type of noble metal, the intrinsic activity (γ) was determined at selected temperatures (between 210 and 300 °C). For the oxidation of both VOC, the intrinsic activities of Pt/TiO_2 and Pd/TiO_2 were found to increase with the metal particle size. In fact, the activity doubles as the average parti-

Table 2
Catalytic activity data expressed as T_{50} (°C), T_{90} (°C) and T_{100} (°C) (temperatures at which 50, 90 and 100% conversion into CO_2 are obtained).

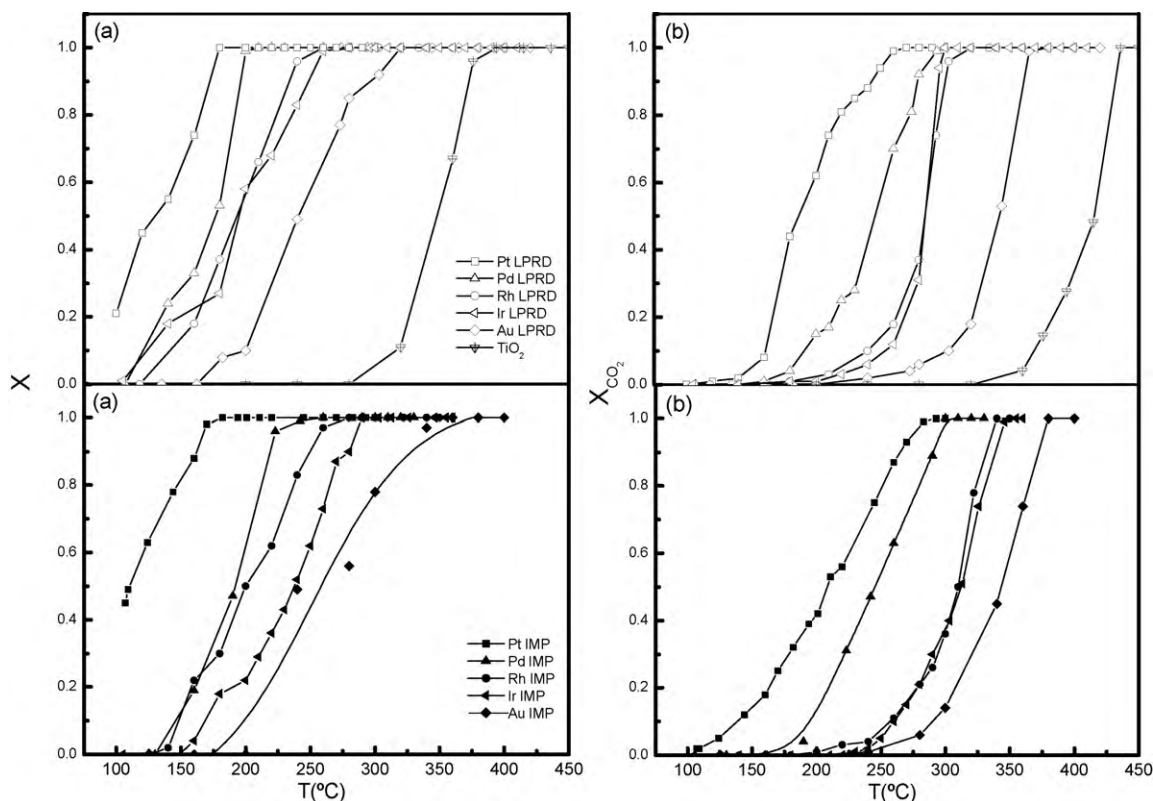| Catalysts	Ethanol			Toluene		
	T_{50}	T_{90}	T_{100}	T_{50}	T_{90}	T_{100}
Pt IMP	208	265	283	196	212	230
Pt LPRD	187	243	260	191	201	210
Pd IMP	245	290	300	226	242	250
Pd LPRD	245	279	294	221	234	240
Ir IMP	312	340	346	–	–	–
Ir LPRD	283	296	300	292	302	313
Rh IMP	310	332	340	–	–	–
Rh LPRD	283	300	316	284	300	310
Au IMP	341	373	380	–	–	–
Au LPRD	341	363	370	372	398	420
TiO_2	413	432	436	403	470	>520

Fig. 4. Light-off curves for ethanol oxidation over supported noble metal catalysts: (a) ethanol conversion (X); (b) conversion into CO_2 (X_{CO_2}).

cle size varies from 3.6 to 5.4 nm (for Pt), or from 4.0 to 7.2 nm (for Pd). These results show that the oxidation of ethanol and toluene over Pt and Pd catalysts is structure sensitive. Considering the Rh and Au catalysts in the oxidation of ethanol, it can be observed that the intrinsic activity slightly decreases with the increase of the average particle size of Rh, while in the case of Au the influence is rather weak, taking into consideration the errors involved.

There are some studies in the literature concerning the effect of the metal particle size on the catalytic combustion of VOC (hydrocarbons, ethyl acetate and benzene) [3,21–23,31]. To the best of our knowledge, no study has been reported on the influence of particle size in the oxidation of toluene and ethanol using these catalysts; particularly, we found no reference to studies concerning titania supported Ir or Rh catalysts. It was observed that the correlation between the catalytic activity and the metal dispersion

Table 3
Specific activities as a function of the catalysts average metal particle size.

Catalyst	d_M[a] (nm)	Ethanol		Toluene	
		T (°C)[c]	γ (s^{-1})	T (°C)[c]	γ (s^{-1})
Pt LPRD	3.6	260	1.05	210	1.05
Pt IMP	5.4		1.89		1.95
Pd LPRD	4.0	294	0.57	240	0.57
Pd IMP	7.2		1.25		1.05
Ir LPRD	1.7	300	0.54	300	0.49
Ir IMP	1.9		0.64		–
Rh LPRD	3.8	300	0.51	300	0.52
Rh IMP	5.2		0.36		–
Au LPRD	4.0[b]	285	0.12	300	0.12
Au IMP	9.1[b]		0.14		–

[a] Obtained by hydrogen chemisorption.
[b] Obtained by TEM.
[c] Selected temperatures for the determination of the intrinsic activities.

depends on the type of VOC, the noble metal and the support. Usually, the oxidation of VOC over Pt supported catalysts is recognized to be structure sensitive [31]. The enhancement of activity on larger crystallites was ascribed to the differences in the nature of the supported active phase. Papaefthimiou et al. [3] studied the oxidation of benzene and ethyl acetate over Pt-based catalysts and they found that the turnover frequency (TOF) strongly increases with the particle size on Pt/Al$_2$O$_3$; on a Pt/TiO$_2$ catalyst this correlation was found to be rather weak compared to the Pt/Al$_2$O$_3$ catalyst.

In both systems (ethanol and toluene), the presence of noble metal decreases the formation of by-products (namely acetaldehyde and acetic acid in ethanol oxidation and CO in toluene oxidation), and increases the CO$_2$ yield. For example, in the presence of the Pt LPRD catalyst, ethanol is completely oxidized into CO$_2$ at 260 °C, while no CO$_2$ was formed at this temperature in the presence of titania only. The CO oxidation experiments (Fig. 2) confirmed these results, since the support is almost unable to convert CO below 350 °C, while in the presence of a noble metal full conversions are already achieved at that temperature, or even below.

By comparing the temperatures for 50, 90 and 100% conversion into CO$_2$, the following performance trend was observed in the oxidation of both VOC (independently of the preparation method): Pt > Pd ≫ Rh ≈ Ir ≫ Au ≫ support (see Table 2). For example, with Pt LPRD, the oxidation of ethanol and toluene into CO$_2$ starts at about 150 °C (Figs. 4 and 5) and complete conversion into CO$_2$ occurs at 260 and 210 °C, respectively (see Table 2). In the presence of Au LPRD, the complete oxidations of ethanol and toluene were achieved at 370 and 420 °C, respectively. This catalytic trend can be explained in terms of the oxidation mechanism. In the literature, it was suggested that the oxidation of VOC over supported noble metal catalysts usually involves the dissociative adsorption of oxygen. Accordingly, the intrinsic activity of each noble metal at a selected temperature was plotted as a function of the dissociative chemisorption energies of oxygen [30], as it was done
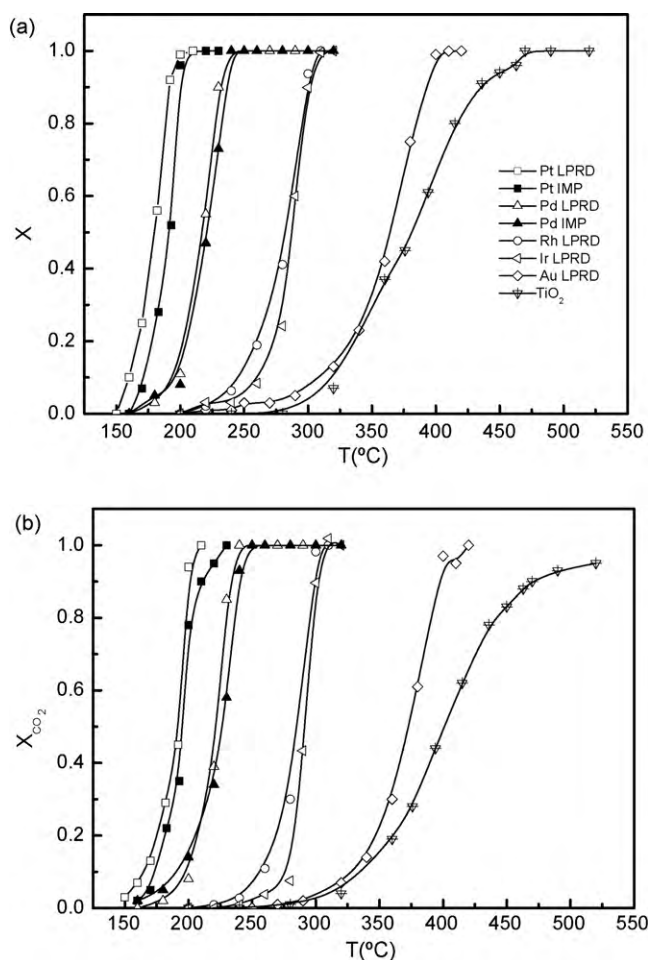
(a)

(b)

Fig. 5. Light-off curves for toluene oxidation over supported noble metal catalysts: (a) toluene conversion (X); (b) conversion into CO_2 (X_{CO_2}).
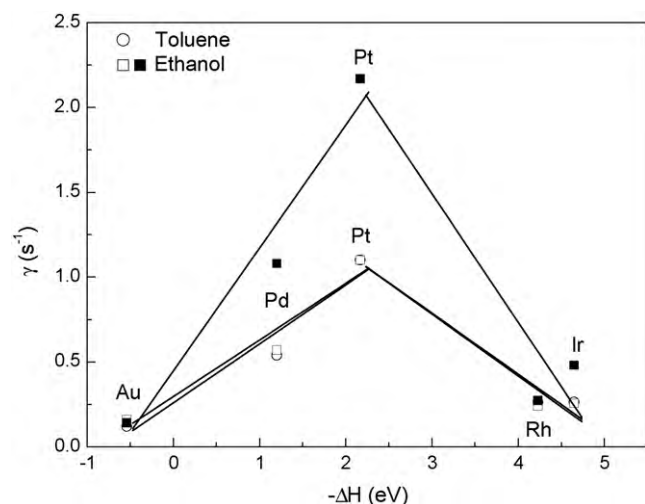

Fig. 6. Volcano-type plot indicating the specific activity at 285 °C in VOC oxidation as a function of oxygen dissociative chemisorption energies on metals. The filled symbols represent the catalysts prepared by incipient wetness impregnation, while the empty symbols represent the catalysts prepared by liquid phase reduction deposition.
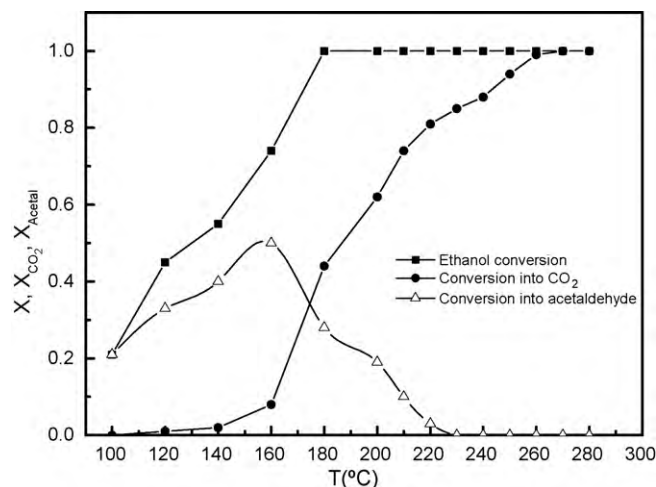

Fig. 7. Light-off curves corresponding to ethanol oxidation on titania supported Pt catalyst (LPRD). Conversion into acetaldehyde (X_{Acetal}) is defined as: $X_{Acetal} = (F_{Acetal}/F_{Ethanol,in})$, where F_{Acetal} is the outlet molar flow rate of acetaldehyde at steady state.

for CO oxidation (see Section 3.2.1). Fig. 6 shows the results thus obtained. As can be seen, typical volcano plots occur, explaining the catalytic trend observed. In particular, it explains the relatively lower performance of gold catalysts in comparison to the other noble metals.
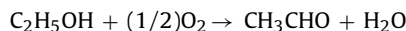
3.2.3. Oxidation of VOC mixtures

Industrial emissions usually contain a mixture of VOC, and not just one single component. Moreover, it has been reported that the oxidation of a VOC in a mixture is different from its single oxidation, due to the interaction of the different species with the catalyst. The mixture effect is very difficult to predict a priori, as either a common inhibition effect or a rare promoting effect could be observed, when the components of the mixture are oxidized [32–38]. Apart from the possible inhibitory or promoting effects, some changes in the selectivity to by-products have also been reported when mixtures of VOC are oxidized [34].

The aim of this section is to study the performance of Pt/TiO₂ (LPRD) in the oxidation of binary mixtures. We will first consider in more detail the complete oxidation of single organic compounds.

3.2.3.1. Single oxidation of ethanol and toluene over titania supported Pt catalyst.
The catalytic performance of the Pt/TiO₂ catalyst in the single oxidation of toluene and ethanol is shown in Figs. 5 and 7, respectively.

Regarding ethanol oxidation (see Fig. 7), it can be seen that acetaldehyde, formed by the partial oxidation of ethanol according to the equation

$$C_2H_5OH + (1/2)O_2 \rightarrow CH_3CHO + H_2O$$

is the primary product below 170 °C. Its production reaches a maximum at ~160 °C, and starts to decrease with temperature increase, down to 0% at 230 °C. On the other hand, the conversion into CO_2 continuously increases with reaction temperature, reaching 100% at 260 °C. During toluene oxidation, no significant amounts of by-products were detected, and $X_{CO_2} \approx X$ (see Fig. 5).

Comparing Figs. 5 and 7, it can be observed that ethanol is slightly more reactive than toluene. These two VOC are completely oxidized at 200 and 210 °C, respectively. However, the complete oxidation into CO_2 occurs at a lower temperature in the case of toluene (see Table 3), which may indicate that the by-products

Fig. 9. Toluene conversion curves alone and in binary mixtures with ethanol, in the presence of titania supported Pt catalyst (LPRD).
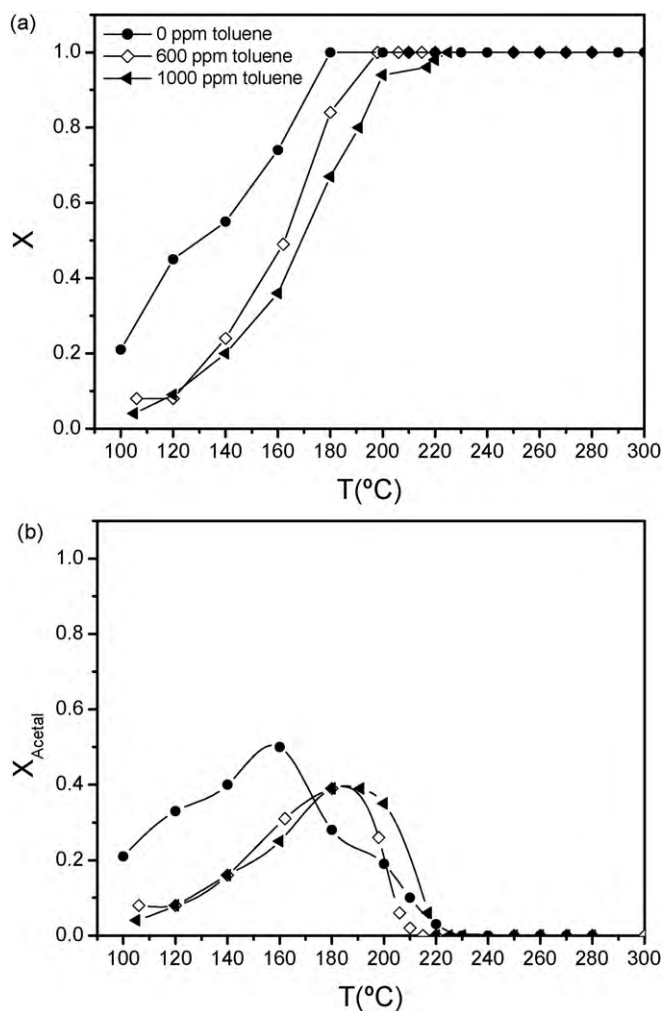
Fig. 8. (a) Ethanol conversion curves alone and in binary mixtures with toluene, in the presence of titania supported Pt catalyst (LPRD). (b) Conversion into acetaldehyde.

formed in the partial oxidation of ethanol (namely acetaldehyde) are less reactive than toluene.

3.2.3.2. Ethanol–toluene mixtures. The results obtained for the oxidation of ethanol and toluene mixtures in the presence of Pt/TiO$_2$ are shown in Figs. 8 and 9. Regarding the effect of toluene on ethanol oxidation (Fig. 8), it can be seen that the presence of toluene inhibits the partial combustion of ethanol (especially at low temperatures), decreasing the acetaldehyde yield. The curves corresponding to the conversion of ethanol and its conversion to acetaldehyde are shifted to higher temperatures as toluene concentration increases. The amount of acetaldehyde formed is smaller when toluene is added to ethanol.

Fig. 9 shows the effect of ethanol concentration on toluene oxidation. It can be observed that the presence of ethanol slightly inhibits toluene combustion, although the effect is not as pronounced as with the addition of toluene to ethanol. Similar results were reported by Burgos et al. [36] for the simultaneous oxidation of toluene and isopropanol over a Pt/Al$_2$O$_3$ catalyst. They found out that toluene inhibits the conversion of 2-propanol to acetone, shifting the light-off curves to higher temperatures, while 2-propanol does not have any significant effect on toluene oxidation. In order to explain these results, adsorption studies of both compounds and subsequent temperature programmed desorption (TPD) and temperature programmed surfa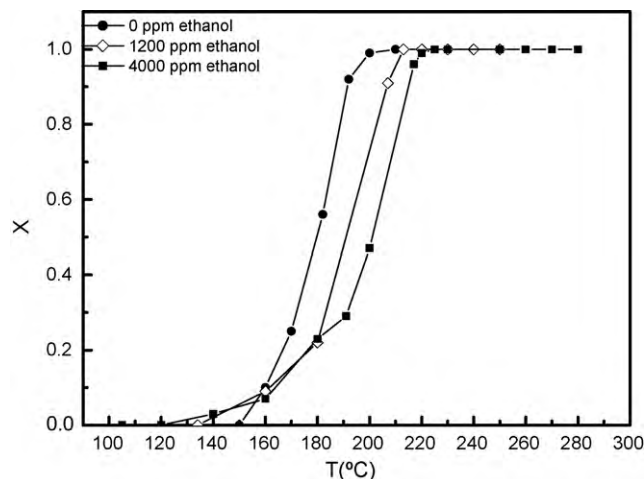ce oxidation (TPSO) experiments were performed by the same authors. They showed that both VOC adsorb on the support, and the adsorption preference is related to the polarity of the VOC. From this result, those authors deduced that toluene reacts mainly in the gas phase with oxygen chemisorbed on the metal surface (Rideal–Eley mechanism). On the other hand, isopropanol is oxidized via acetone formation over the catalyst surface, by a two-centre mechanism involving alcohol chemisorbed on alumina and oxygen chemisorbed on Pt. In summary, the reactivity is mainly affected by the competition for the oxygen atoms chemisorbed on the Pt particles. Although the support used in our work is different (TiO$_2$) from that reported by Burgos et al. (Al$_2$O$_3$) [31], we believe that the results obtained by these authors can help us to interpret our own findings. Moreover, isopropanol is not that much different from ethanol in terms of polarity (authors report the formation of acetone instead of acetaldehyde as we found in our own work) and toluene was also used in the mentioned work. Therefore, we believe that a similar mechanism can take place in the present case.

4. Conclusions

The main conclusions that can be drawn from this study are:

- LPRD is a suitable method for the preparation of highly dispersed supported noble metal catalysts, which are very active for the total oxidation of CO and VOC.
- The preparation method does not change the catalytic trend in VOC oxidation, but it does in CO oxidation. The following performance trend was observed for VOC oxidation for both preparation methods: Pt > Pd ≫ Rh ≈ Ir ≫ Au ≫ support. For CO oxidation, the trend for the catalysts prepared by LPRD is Au ≫ Pt > Pd > Rh > Ir, while for IMP samples is Rh > Ir > Pd ≈ Pt > Au.
- The dispersion of the metal phase has an important effect on the performance of the catalysts towards total oxidation of CO and VOC (especially in the case of Au in CO oxidation).
- The oxidation reactions of ethanol and toluene in the presence of Pt or Pd catalysts are structure sensitive.
- In the catalytic oxidation of mixtures over Pt/TiO$_2$ it was observed that toluene and ethanol have a mutual inhibitory effect. However, this effect is much more evident in the case of ethanol.

Acknowledgements

References

[1] J.J. Spivey, Ind. Eng. Chem. Res. 26 (1987) 2165.
[2] J.E. Sawyer, M.A. Abraham, Ind. Eng. Chem. Res. 33 (1994) 2084.
[3] P. Papaefthimiou, T. Ioannides, X.E. Verykios, Appl. Catal. B-Environ. 15 (1998) 75.
[4] E.M. Cordi, J.L. Falconer, Appl. Catal. A-Gen. 151 (1997) 179.
[5] G.L. Dong, J.G. Wang, Y.B. Gao, S.Y. Chen, Catal. Lett. 58 (1999) 37.
[6] T. Mitsui, T. Matsui, R. Kikuchi, K. Eguchi, Top. Catal. 52 (2009) 464.
[7] W.B. Li, J.X. Wang, H. Gong, Catal. Today 148 (2009) 81.
[8] N. Bion, F. Epron, M. Moreno, F. Marino, D. Duprez, Top. Catal. 51 (2008) 76.
[9] G.C. Bond, D.T. Thompson, Gold Bull. 33 (2000) 41.
[10] E.D. Park, D. Lee, H.C. Lee, Catal. Today 139 (2009) 280.
[11] M. Skoglundh, E. Fridell, Top. Catal. 28 (2004) 79.
[12] S.A.C. Carabineiro, D.T. Thompson, in: E.U. Heiz, U. Landman (Eds.), Nanocatalysis, Springer-Verlag, Berlin, Heidelberg, New York, 2007, pp. 377–489.
[13] S.A.C. Carabineiro, D.T. Thompson, in: C. Corti, R. Holliday (Eds.), Gold: Science and Applications, CRC Press, Taylor and Francis Group, Boca Raton, London, New York, 2010, pp. 89–122.
[14] S.A.C. Carabineiro, A.M.T. Silva, G. Dražić, P.B. Tavares, J.L. Figueiredo, 2010, doi:10.1016/j.cattod.2009.12.017.
[15] P. Papaefthimiou, T. Ioannides, X.E. Verykios, Catal. Today 54 (1999) 81.
[16] C. Della Pina, N. Dimitratos, E. Falletta, M. Rossi, A. Siani, Gold Bull. 40 (2007) 67.
[17] M.I. Dominguez, M. Sanchez, M.A. Centeno, M. Montes, J.A. Odriozola, J. Mol. Catal. A-Chem. 277 (2007) 145.
[18] C. Gennequin, M. Lamallem, R. Cousin, S. Siffert, F. Aissi, A. Aboukais, Catal. Today 122 (2007) 301.
[19] S.Y. Liu, S.M. Yang, Appl. Catal. A-Gen. 334 (2008) 92.
[20] G. Bond, D. Thompson, Gold Bull. 42 (2009) 247.
[21] P. Briot, A. Auroux, D. Jones, M. Primet, Appl. Catal. 59 (1990) 141.
[22] V. Labalme, E. Garbowski, N. Guilhaume, M. Primet, Appl. Catal. A: Gen. 138 (1996) 93.
[23] K. Otto, Langmuir 5 (1989) 1364.
[24] Y. Sunagawa, K. Yamamoto, H. Takahashi, A. Muramatsu, Catal. Today 132 (2008) 81.
[25] P.C. Aben, J. Catal. 10 (1968) 224.
[26] V.P. Santos, M.F.R. Pereira, J.J.M. Órfão, J.L. Figueiredo, Top. Catal. 52 (2009) 470.
[27] M. Lamallem, H. El Ayadi, C. Gennequin, R. Cousin, S. Siffert, F. Aissi, A. Aboukais, Catal. Today 137 (2008) 367.
[28] S. Ivanova, W. Pitchon, Y. Zimmermann, C. Petit, Appl. Catal. A-Gen. 298 (2006) 57.
[29] R. Zanella, L. Delannoy, C. Louis, Appl. Catal. A-Gen. 291 (2005) 62.
[30] T. Bligaard, J.K. Norskov, S. Dahl, J. Matthiesen, C.H. Christensen, J. Sehested, J. Catal. 224 (2004) 206.
[31] T.F. Garetto, C.R. Apesteguia, Appl. Catal. B-Environ. 32 (2001) 83.
[32] J. Hermia, S. Vigneron, Catal. Today 17 (1993) 349.
[33] J. Tsou, P. Magnoux, M. Guisnet, J.J.M. Órfão, J.L. Figueiredo, Appl. Catal. B-Environ. 57 (2005) 117.
[34] F.N. Aguero, B.P. Barbero, L. Gambaro, L.E. Cadus, Appl. Catal. B-Environ. 91 (2009) 108.
[35] V. Blasin-Aubé, J. Belkouch, L. Monceaux, Appl. Catal. B-Environ. 43 (2003) 175.
[36] N. Burgos, M. Paulis, M.M. Antxustegi, M. Montes, Appl. Catal. B-Environ. 38 (2002) 251.
[37] J.I. Gutierrez-Ortiz, B. de Rivas, R. Lopez-Fonseca, J.R. Gonzalez-Velasco, Appl. Catal. B-Environ. 65 (2006) 191.
[38] P.-O. Larsson, A. Andersson, Appl. Catal. B-Environ. 24 (2000) 175.